CORROSION SCIENCE AND TECHNOLOGY, Vol.24, No.3(2025), pp.175~183 pISSN 1598-6462 / eISSN 2288-6524
[Research Paper] DOI: https://doi.org/10.14773/cst.2025.24.3.175

Evaluation of Corrosion Resistance of Aluminium-Silicon Carbide Composites for Thermal Application

Baydaa Jaber Nabhan, Lubna Ghalib†, and Manal Hameed Jasem

Materials Engineering Department, Mustansiriyah University, Baghdad-Iraq

(Received October 18, 2024; Revised January 18, 2025; Accepted February 03, 2025)

Aluminium-silicon carbide (Al-SiC) has garnered attention recently due to its advantageous features. Effects of uniform corrosion and pitting corrosion susceptibility of Al-SiC composites in HCl solution were investigated using cyclic potentiodynamic polarization for thermal application. Surface morphology of Al-SiC composites was examined by scanning electron microscope (SEM) and energy Dispersive spectroscopy (EDS). This study was complemented by examining elemental compositions of various composites through surface analysis methods. Results revealed that composites sintered for 2 hours at 550 °C exhibited a decrease in the rate of uniform corrosion and a diminished susceptibility to pitting corrosion when the solution temperature was elevated. Extending the sintering time for composite to 3 hours led to an enhancement in uniform corrosion, while concurrently mitigating the incidence of pitting corrosion. Uniform corrosion of sintered composites showed a significant dependence on sintering time with increasing temperature. Sintering time can potentially affect grain size, resulting in a corrosion behavior.

Keywords: *Al-SiC composites, Cyclic polarization, Powder metallurgy, Temperature, Pitting corrosion*

1. Introduction

Aluminium reinforced with silicon carbide represents a significant area of study due to its combination of desirable mechanical and physical qualities relative to conventional materials. The pitting corrosion of composites can negate enhancements in their mechanical qualities and restrict their applicability. Aluminium-SiC composites are increasingly used in aerospace components, the automotive industry, and precision machinery; electronic packing owing to their excellent thermal conductivity of Al-SiC makes it suitable for use in systems that require thermal control, such as radiators and heat exchangers. Nonetheless, corrosion of Al-SiC composites transpires and constitutes a significant issue in the thermal system. The Al-SiC composite is subjected to a broad temperature range and intricate components [1,2]. Typical heat transfer fluids exhibit little aggressiveness, unless in cases of contamination or exposure to elevated temperatures (degradation). The composite Al-SiC experiences pronounced pitting corrosion due to the substantial decrease in its corrosion resistance attributed to the presence of chloride ions. The resistance to pitting corrosion was examined using cyclic potentiodynamic polarization. The hysteresis observed in the cyclic polarization curve can yield insights into the mechanisms of pitting corrosion and the efficiency which a passive film can regenerate. Pitting corrosion will happen when the current density observed during the anodic curve in the reverse scan is greater than that of the forward scan at the same anodic potential, according to a basic principle of this approach. Research by Silverman [3] as well as Beavers *et al.* [4] provide more information about this phenomenon, which is called "negative hysteresis" [5]. The cyclic potentiodynamic polarization technique is an appropriate method for examining the initiation of passivity, the breakdown of the oxide coating, susceptibility to re-passivation, as well as the quantification of pitting corrosion rates, owing to its extensive range of scanning potential [6,7].

Numerous studies have been conducted on the corrosion resistance of composites in various environments. Additional studies examine the corrosion behavior of aluminum matrix composites. Certain research [8] has shown that the formation of electrochemical interactions between reinforcement particles and the composite matrix accelerates the corrosion of aluminium base composites

†Corresponding author: lubnaghalib81@uomustansiriyah.edu.iq

and causes a decrease in corrosion resistance due to galvanic interactions between reinforcements. Additional types of corrosion, including selective and localized corrosion (such as crevice and pitting corrosion), may also arise, restricting the use of certain Al-based alloys [9-12]. The susceptibility to pitting corrosion, the potential of pitting, and the morphology of pitting for aluminum matrix composites within sodium chloride solutions were also documented [13-15].

Under elevated temperature conditions, SiC-reinforced aluminum composites exhibit more pits in comparison to their unreinforced equivalents. While it has been proposed that silicon carbide actively contributes to composite corrosion by promoting pitting initiation, this assertion has not been definitively proven. This study aims to assess the resistance to uniform and pitting corrosion of Al-SiC composites by the cyclic potentiodynamic polarization technique in an aqueous medium of 0.5 M HCl at different sintering times and also the accurate interpretation of its results to predict Al-SiC pitting corrosion behavior appropriately.

2. Experimental

2.1 Materials and composite fabrication

Aluminium powder, characterized by an average particle size of 75 μm and a purity of 99.5% supplied by HiMedia Laboratories Pvt. Ltd. and SiC powders possessing an average particle size < 80 μm and a purity of 99% were the materials that served as the foundation for this study undertaking. The law of mixtures was employed to calculate the quantities of mixed powders necessary to manufacture SiC particle-reinforced composites (11 mm in diameter and 30 mm in height). The aluminium and silicon carbide powders were combined in an electric parallel mixer at a velocity of 70 rpm for two hours to guarantee thorough amalgamation. Our prior study reported the accurate and uniform distribution of SiC particles within the aluminum matrix [16]. The mixed powders (90% Al and 10% SiC) and (80% Al and 20% SiC) were poured and pressed in a steel die under a pressure of 146 Mpa and then sintered in a high-vacuum tubular furnace. The resultant composites underwent sintering at a temperature of 550 ºC in a vacuum for 2 and 3 hours, respectively.

2.2 Corrosion test

The samples were sequentially polished using silicon carbide grinding paper with abrasive sizes of 2000 grit. The potentiodynamic polarization electrochemical technique was employed to conduct corrosion testing on the fabricated composites. A Gamry Instruments potentiostat, accompanied by Gamry software, served as the testing apparatus for the corrosion experimentation. The samples were thoroughly cleaned to eliminate the initial oxide layer before the electrochemical testing. The Al-SiC electrode was fabricated before immersion in a 0.5 M HCl test solution, as reported in previously published research [2,16]. To evaluate the impact of environmental temperature on the electrochemical behavior of the composites, the test electrodes were immersed in the 0.5 M HCl test solution for about 1500 seconds to stabilize the open-circuit potential before each measurement. A three-electrode corrosion cell configuration was used for all corrosion experiments. The experimental setup consisted of the sample functioning as the working electrode, a saturated calomel electrode designed as the reference electrode, and a graphite rod serving as the counter electrode. Potentiodynamic polarization assessments were conducted at a scan rate of 2.5 mV/s, with the initial potential ranging between -0.25 V and +0.25 V (vs. SCE). The tests were replicated to ensure the accuracy of the collected data. The ASTM standard procedure determined the corrosion rate for the samples according to the equation (1) below [17]:

$$CR = \frac{Ki_{corr}E_W}{\mu A} \quad (1)$$

CR represents the corrosion rate measured in mm/yr, K constant valued at 3.27×10^{-3} mm/(A cm year), i_{corr} denotes the corrosion current expressed in A, ρ signifies the density of the composite in g/cm^3, E_w indicates the equivalent weight of the composite in g and A is the area of the exposure surface in cm^2. The corrosion resistance (R_p) was respectively calculated according to the following equation (2) [18]:

$$R_p = \frac{\Delta E}{\Delta i} = \left(\frac{\beta_c \beta_a}{2.3 i_{corr}(\beta_c + \beta_a)}\right) \quad (2)$$

Where R_p is the polarization resistance in ohms, all the

corrosion tests were carried out in a 0.5 M HCl environment at 25, 45, and 65 ºC. Scanning electron microscopy (SEM) and energy dispersive spectroscopy (EDS) characterize the surface morphology of Al-SiC composites. The surface morphology was employed to examine the composite's microstructural states after the corrosion tests.

3. Results and discussion

3.1 Cyclic potentiodynamic polarization analyses

The cyclic polarization curves of the Al-10%SiC and Al-20%SiC composites are present in Fig. 1 and Fig. 2, respectively. The composites were fabricated through powder metallurgy technique at a sintering temperature of 550 ºC for 2 hours and exposed to 0.5 M HCl at 25, 45, and 65 ºC. The reduction of hydrogen ions and oxygen represent the most probable partial cathodic reactions of corrosion according to equations:

$$2H^{+} + 2e^{-} \rightarrow H_2 \quad (3)$$

$$O_2 + 2H_2O + 4e^{-} \rightarrow 4OH^{-} \quad (4)$$

The uniform corrosion of composites increases with increasing temperature from 25 ºC to 45 ºC. This phenomenon can be ascribed to the enhanced diffusion rate of hydrogen that occurs with an increase in temperature, alongside the elevation in activation energy of the acidic solution, which facilitates the hydrogen evolution process [11]. As the oxygen reaction proceeds, an oxide film forms on the electrode surface [19]. Therefore, the composite demonstrated elevated corrosion resistance and spontaneous passivity in proximity to the corrosion potential zone. It is seen from Fig. 1 that at a temperature of 25 ºC, the composite would be passivated in 0.5 M HCl. The passive region of the composite demonstrated significant stability, appearing as a nearly horizontal line parallel to the x-axis, this phenomenon signifies exceptional corrosion resistance. Such resistance can be attributed to the minimal presence of SiC in comparison to that depicted in Fig. 2 at room temperature.

As the solution temperature was elevated to 45 ºC, both anodic dissolution and cathodic current density exhibited an increase, while the corrosion potential shifts to more

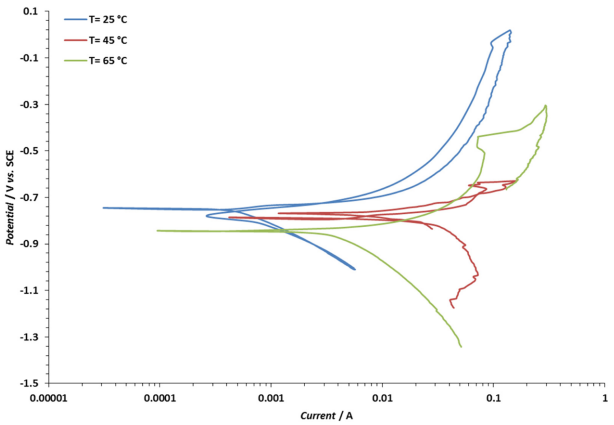

Fig. 1. potentiodynamic cyclic polarization scan of Al-10%SiC composite sintered at 550 ºC for 2 hours in 0.5 M HCl solution

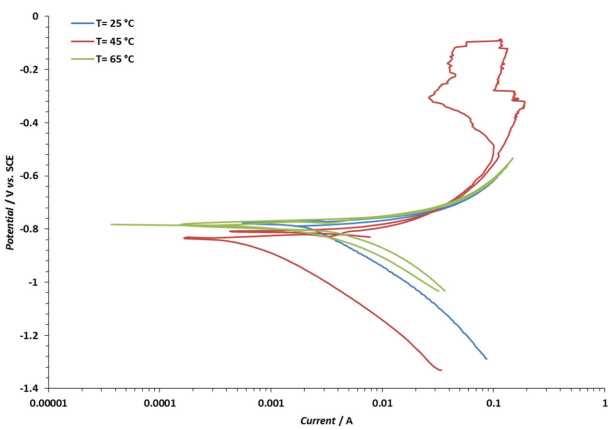

Fig. 2. potentiodynamic cyclic polarization scan of Al-20%SiC composite sintered at 550 ºC for 2 hours in 0.5 M HCl solution

negative direction. The kinetics of electrochemical reactions accelerate, consequently resulting in an amplification of uniform corrosion. At this elevated temperature, localized acidic sites are established, which culminates in the development of a defective and porous oxide layer on the electrode surface [19]. This is indicative of the emergence of metastable pitting corrosion, stemming from the sequential formation and repassivation of microscale pits [20,21]. These metastable pits grow and repassivate quickly. it is obvious from cyclic polarization curve at temperature 45 ºC and 65 ºC, local loss film breakdown at breakdown potential (E_{pit}). Propagation and growth of pitting corrosion are induced by alterations in chemical composition of the solution within the pits. The environment inside the pits becomes

increasingly aggressive and acidic due to the influx of Cl^- ions and the hydrolysis of intermetallic compounds contained within the pits.

The findings indicate that an elevation in the temperature of composites sintered for 2 hours from 45 ºC to 65 ºC inhibits the hydrogen and oxygen reactions and enhances the anodic oxidation processes, thereby signifying a reduction in the uniform corrosion rate of the composite. Furthermore, it has been observed that the pitting potential shifts toward a more positive direction, reflecting an enhancement in the resistance to pitting corrosion.

In all examined temperatures, the cyclic polarization curves recorded for the composites showed a hysteresis loop, indicating that the composites possess the capability to repassivate following the breakdown of the passive film at the repassivation potential (E_{rp}) [22]. Hence, the data clearly indicate that an increase in temperature inhibits both uniform and pitting corrosion of composites sintered at 550 ºC for 2 hours in a 0.5 M HCl solution.

Fig. 3 and Fig. 4 showed the cyclic polarization curves obtained from the composites with 10 wt% and 20 wt% SiC subjected to sintering at temperature 550 ºC for 3 hours, and tested in a 0.5 M HCl solution, respectively. An increase in duration of sintering resulted in a more refined grain size distribution, as the grains attained a more uniform morphology and dimensions. Furthermore, the porosity of the composites that underwent sintering for 3 hours was lower, resulting in a reduced specific surface area that is vulnerable to uniform corrosion [23]. This effect becomes particularly pronounced when the solution temperature is raised from 25 ºC to 45 ºC. Consequently, the formation of enriched and more compact particle boundaries established an effective barrier against corrosion attacks, which contributed to the additional reduction in the corrosion rate of the composite. This observation substantiates the assertion that elevating the solution temperature to 45 ºC, in conjunction with prolonged sintering times of 3 hours for the composite, diminishes its uniform corrosion while simultaneously enhancing the pitting corrosion of the composite [24]. The corrosion rate exhibited a gradual increase with escalation of the solution temperature from 45 ºC to 65 ºC, attributable to the dissolution of the oxide film and the segregation of corrosion products at particle boundaries,

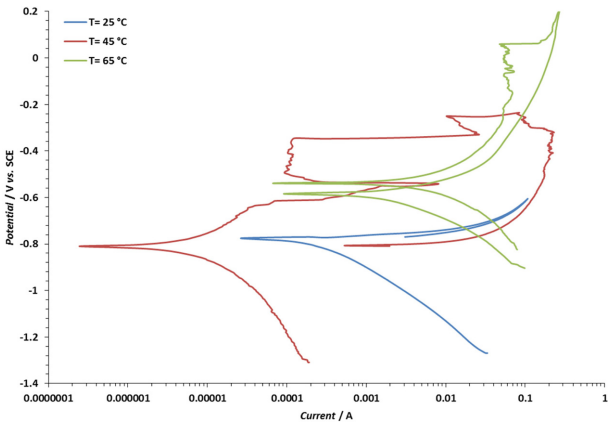

Fig. 3. potentiodynamic cyclic polarization scan of Al-10%SiC composite sintered at 550 ºC for 3 hours in 0.5 M HCl solution

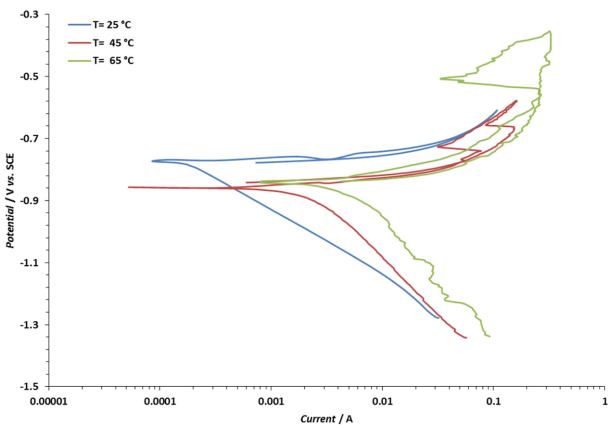

Fig. 4. potentiodynamic cyclic polarization scan of Al-20%SiC composite sintered at 550 ºC 3 hours in 0.5 M HCl solution

which facilitated the ingress of Cl^- ions, thereby exacerbating the galvanic corrosion between the boundaries and the aluminium matrix [25]. The elevation of temperature to 65 ºC catalyzes the rates of migration and diffusion of composite species, thereby fostering the formation of pits and consequently amplifying the rate of pitting propagation. All these occurrences facilitate the incursion of the aggressive Cl- anion, which undermines the passivity of the oxide film, culminating in the emergence of intense pitting corrosion and distinctly illustrating the propagation of corrosion attacks along the grain boundaries, thereby resulting in the formation of an unstable passivation layer which, in turn, effectively penetrates and degrades the composite [25].

Table 1. The electrochemical parameters for composite obtained from potentiodynamic cyclic polarization in 0.5 M HCl solution

composites	T (°C)	E_{corr} (mV)	i_{corr} (mA)	E_{pit} (mV)	E_{rp} (mV)	R_P (Ω)	CR (mm/y)
Al-10%SiC sintered for 2 hours	25	-744.0	0.652	-	-705.1	30.33	10.59
	45	-787.0	13.90	-731.1	-778.3	1.69	225.70
	65	-844.0	4.96	-438.9	-818.2	6.31	80.60
Al-10%SiC sintered for 3 hours	25	-776.0	0.161	-	-	51.59	2.544
	45	-811.0	0.0125	-644.7	-	5915	0.2028
	65	-585.0	1.76	-	-554.4	13.11	28.65
Al-20%SiC sintered for 2 hours	25	-835.0	0.798	-	-787.0	23.5	12.96
	45	-857.0	1.900	-301.2	-735.8	8.5	30.86
	65	-639.0	0.454	-	-783.0	35.4	7.378
Al-20%SiC sintered for 3 hours	25	-856.0	3.340	-	-	14.5	54.18
	45	-783.0	1.510	-727.3	-769.9	9.12	24.47
	65	-840.0	6.430	-508.0	-565.7	5.4	104.4

The electrochemical parameters derived from the cyclic polarization curves of composites in 0.5 M HCl solution are listed in Table 1. The parameters included corrosion potential (E_{corr}), corrosion current (i_{corr}), pitting potential (E_{pit}), repassivation potential (E_{rp}), corrosion resistance (R_p), and corrosion rate (CR). It can be seen from Tables 1 that uniform corrosion of composites sintered for 2 hours increased significantly as temperature increased from 25 °C to 45 °C. in this part, the diffusion of corrosion species were accelerated when temperature increased. Some small cavities still existed in the corrosion film formed at 45 °C, although corrosion film at 45 °C possessed better protectiveness than that at 25 °C. The protection of corrosion film on the composite was still insufficient compared to the attack of corrosion environment. As temperature increased to 65 °C, the uniform corrosion decreased sharply. However, the oxygen concentrations decreased slightly lead to active oxidation of SiC as temperature increased from 45 °C to 65 °C [26]. On the other hand, the corrosion film became more even and continuous. Furthermore, the corrosion film resistance increased rapidly when temperature exceeded 65 °C. As a result, the content of corrosive ions at the interface between composite and corrosion films would decrease, resulting in decrease in the uniform corrosion. It could be concluded that sintering times of composites have a greater influence on film formation and decrease the uniform and pitting corrosion.

3.2 Surface Morphology for composite

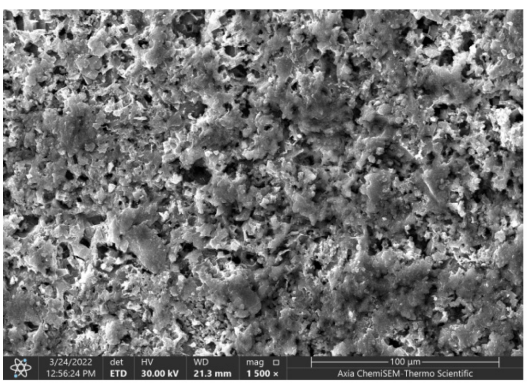

Element	Weight %
C	26.3
O	8.3
Al	62.1
Si	1.0
Cl	0.2
Fe	0.3
Sb	1.8

Fig. 5. SEM-EDS analysis of surface morphology for Al-10%SiC sintered at 550 °C for 2 hours after potentiodynamic polarization test at 65 °C

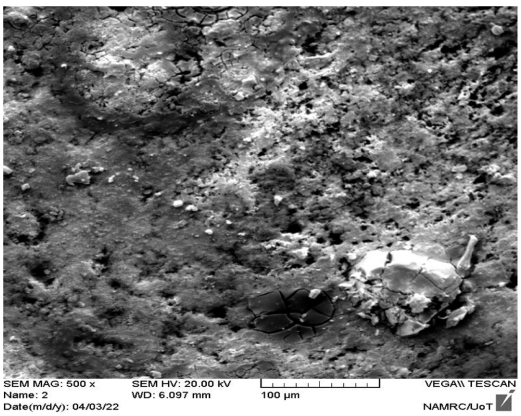

Element	Weight %
Al	58.3
Sb	15.3
O	11.4
C	10.0
S	3.6
Si	1.3

Fig. 6. SEM-EDS analysis of surface morphology for Al-10%SiC sintered at 550 °C for 3 hours after potentiodynamic polarization test at 65 °C

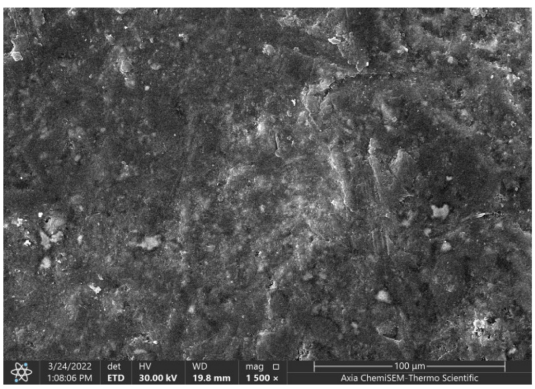

Element	Weight %
C	14.4
O	14.8
Na	0.2
Al	63.0
Si	1.1
S	0.9
Cl	0.3
Sb	5.4

Fig. 7. SEM-EDS analysis of surface morphology for Al-20%SiC sintered at 550 °C for 2 hours after potentiodynamic polarization test at 65 °C

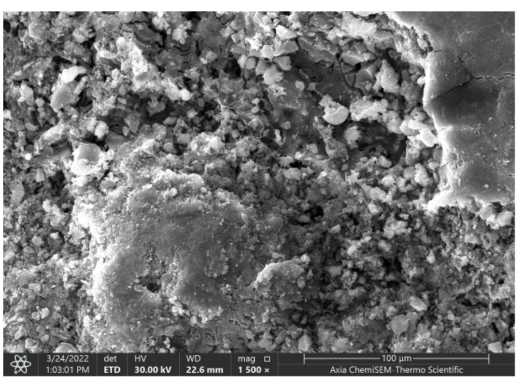

Element	Weight %
C	11.4
O	41.0
Al	38.1
Si	0.1
S	1.2
Cl	0.2
Fe	0.5
Sb	7.3

Fig. 8. SEM-EDS analysis of surface morphology for Al-20%SiC sintered at 550 °C for 3 hours after potentiodynamic polarization test at 65 °C

After the potentiodynamic polarization test, the corrosion products were observed and deposited on the surface of the composite, as shown in Fig.s 5 ~ 8. The chemical compositions of the corrosion products were analyzed with the aid of SEM and EDS. It is clear from the SEM images presented in Fig.s 5 ~ 8 that the surface exhibits a layer of corrosion product along with numerous pits. The corrosion products are characterized by the presence of a developed oxide layer on the surface. This assertion was corroborated by the elemental composition discerned on the surface through energy-dispersive spectroscopy analysis. The elevated concentrations of aluminium and oxygen on the surface indicate that the compound generated is likely aluminium oxide, Al_2O_3.

When comparing the surface of the composite Al-20%SiC, as illustrated in Fig. 7, to the surfaces of other composites shown in Fig.s 5 and 8, the scanning electron microscopy imagery reveals a surface that is predominately coated with a substantial layer of corrosion products, exhibiting a reduced number of pits [27].

Surface characterization indicated that the Al-SiC electrode experienced pitting corrosion following the potentiodynamic experiments. The onset of pit formation was correlated with the active sites and the localized dissolution of the composite matrix surrounding the secondary phase particles. It is well established that corrosion preferentially commences at the interface between the particulate matter and the matrix. A phenomenon known as micro-galvanic coupling exists, leading to the preferred dissolution of composites. The corrosion process was facilitated by the localized cathodes that intermetallic particles provided. Pitting occurred when aluminum was dissolved concomitantly with intermetallic particles that had become dislodged from the aluminum matrix. The aluminum exhibited increased dissolution activity at higher temperatures, resulting in enhanced active dissolution and a larger area of dissolved aluminum. There was an increase in the micro-galvanic coupling effect. The nearby pits merged to create a larger pit, reducing the number of pits at varying temperatures. Consequently, the pit size increased, and the aluminum electrode tended to have uniform corrosion [28].

4. Conclusion

Thermal processing has been shown to significantly influence the corrosion resistance of Al-SiC composites when exposed to hydrochloric acid (HCl) environments. The Al-10%SiC and Al-20%SiC composites subjected to testing in a 0.5 M HCl solution at temperatures of 25, 45, and 65 °C exhibit notable variations in their corrosion resistance. Within an acidic medium, elevated temperatures can affect the corrosion mechanisms by facilitating the electrochemical reactions (both anodic and cathodic) and regulating the movement of reactants toward the sites of reaction. Higher temperatures lead to an increase in the formation of pits, resulting in a discernible pattern of uniform corrosion. The effect of temperature on both composite variants, which were sintered for duration of 2 hours, effectively minimized both pitting and uniform corrosion phenomena. This enhancement in corrosion behavior can be attributed to the development of thicker and more consistent protective oxide layers. An extension of the sintering time to 3 hours correspondingly improved the corrosion characteristics of the composite. It may be inferred that the sintering duration of the composites exerts a more pronounced influence on the integrity of the corrosion barrier, thereby reducing uniform corrosion as the temperature continues to rise.

Acknowledgements

The authors would like to thank the Mustansiriyah University (www.uomustansiriyah.edu.iq) Baghdad-Iraq for its support in the present work.

References

1. C. Xin, T. Wenming, L. Songmei, Y. Mei, L. Jianhua, Effect of temperature on corrosion behavior of 3003 aluminum alloy in ethylene glycol–water solution, *Chinese Journal of Aeronautics*, **29**, 1142 (2016). Doi: https://doi.org/10.1016/j.cja.2015.12.017
2. S.M. Mahdi, and L. Ghalib, Corrosion Behavior of Al/SiC Composite Prepared by Powder Metallurgy in Chloride Environments, *Journal of Bio-and Tribo-Corrosion*, **8**, 8 (2022). Doi: https://doi.org/10.1007/s40735-021-00612-6
3. D. C. Silverman, Tutorial on cyclic potentiodynamic polarization technique, *Proc. NACE CORROSION Conf.*, p. 98299, San Diego, California (1998). https://onepetro.org/NACECORR/proceedings-abstract/CORR98/All-CORR98/127779
4. J. A. Beavers, N. G. Thompson, and C. L. Durr, Unique interpretations of potentiodynamic polarization technique, *Proc. NACE CORROSION Conf.*, p. 98300, San Diego, California (1998). https://onepetro.org/NACECORR/proceedings-abstract/CORR98/All-CORR98/127701
5. A. K. Sfikas, and A. G. Lekatou, Electrochemical behavior of Al–Al_9Co_2 alloys in sulfuric acid, *Corrosion and Materials Degradation*, **1**, 12 (2020). Doi: https://doi.org/10.3390/cmd1020012
6. S. Esmailzadeh, M. Aliofkhazraei, and H. Sarlak, Interpretation of cyclic potentiodynamic polarization test results for study of corrosion behavior of metals: a

review, *Protection of metals and physical chemistry of surfaces*, **54**, 976 (2018). Doi: https://doi.org/10.1134/S207020511805026X

7. L. Ghalib, A. K. Muhammad, and S. M. Mahdi, Study the Effect of Adding Titanium Powder on the Corrosion Behavior for Spot Welded Low Carbon Steel Sheets, *Journal of Inorganic and Organometallic Polymers and Materials*, **31**, 2665 (2021). Doi: https://doi.org/10.1007/s10904-020-01863-5
8. R. M. Raouf, L. Ghalib, and A. K. Muhammad, Mechanical Performance and Corrosion Behaviour of Aluminum7075 Reinforced by Nano-Titanium dioxide, *Baghdad Science Journal*, **21**, 3013 (2024). Doi: https://doi.org/10.21123/bsj.2024.9690
9. H. S. Abdo, U. A. Samad, J. A. Mohammed, S. A. Ragab and A. H. Seikh, Mitigating corrosion effects of Ti-48Al-2Cr-2Nb alloy fabricated via electron beam melting (EBM) technique by regulating the immersion conditions, *Crystals*, **11**, 889 (2021). Doi: https://doi.org/10.3390/cryst11080889
10. H. S. Abdo, A. H. Seikh, A. Fouly, S. A. Ragab, Synergistic strengthening effect of reinforcing spark plasma sintered Al-Zn-TiC nanocomposites with TiC nanoparticles, *Crystals*, **11**, 842 (2021). Doi: https://doi.org/10.3390/cryst11080842
11. K. H. W. Seah, M. Krishna, V. T. Vijayalakshmi, J. Uchil, Effects of temperature and reinforcement content on corrosion characteristics of LM13/albite composites, *Corrosion Science*, **44**, 761 (2002). Doi: https://doi.org/10.1016/S0010-938X(01)00074-9
12. L. Ghalib, , S. M. Mahdi, and A. H. Majeed, Hardness and corrosion behavior of Al-Ti-Cu alloys fabricated by powder metallurgy technique, *Emergent Materials*, **7**, 1191 (2024). Doi: https://doi.org/10.1007/s42247-024-00665-6
13. P. P. Trzaskoma, Pit morphology of aluminum alloy and silicon carbide/aluminum alloy metal matrix composites, *Corrosion*, **46**, 402 (1990). Doi: https://doi.org/10.5006/1.3585124
14. G. E. Kiourtsidis, and S. M. Skolianos, Pitting corrosion of artificially aged T6 AA2024/SiCp composites in 3.5 wt.% NaCl aqueous solution, *Corrosion Science*, **49**, 2711 (2007). Doi: https://doi.org/10.1016/j.corsci.2006.10.008
15. G. Kiourtsidis, and S. M. Skolianos, Corrosion behavior of squeeze-cast silicon carbide-2024 composites in aerated 3.5 wt.% sodium chloride, *Materials Science and Engineering: A*, **248**, 165 (1998). Doi: https://doi.org/10.1016/S0921-5093(98)00494-8
16. S. M. Mahdi, and L. Ghalib, Effect of sintering temperature and time on corrosion characteristics of aluminum matrix composites, *Journal of Electrochemical Science and Engineering*, **13**, 1015 (2023). Doi: https://doi.org/10.5599/jese.1891
17. S. R. Oke, O. O. Ige, O. E. Falodun, B. A. Obadele, M. R. Mphahlele, P. A. Olubambi, Influence of sintering process parameters on corrosion and wear behaviour of SAF 2205 reinforced with nano-sized TiN, *Materials Chemistry and Physics*, **206**, 166 (2018). Doi: https://doi.org/10.1016/j.matchemphys.2017.12.018
18. S. M. Almotairy, E. S. M. Sherif, N. H. Alharthi, H. S. Abdo, H. F. Alharbi, M. Luqman, Influence of milling route on the corrosion passivation of Al-2% SiC nanocomposites in chloride solutions, *Crystals*, **11**, 1231 (2021). Doi: https://doi.org/10.3390/cryst11101231
19. Q. Li, J. O. Jensen, and N. Bjerrum, Chemistry, electrochemistry, and electrochemical applications: Aluminum, *Encyclopedia of Electrochemical Power Sources*, **2009**, 695 (2009). Doi: https://doi.org/10.1016/B978-044452745-5.00951-5
20. Y.-H. Chen, PhD. Dissertation , UNSW University, Sydney (2018).
21. C. Chatillon, and F. Teyssandier, Thermodynamic assessment of the different steps observed during SiC oxidation, *Journal of the European Ceramic Society*, **42**, 1175 (2022). Doi: https://doi.org/10.1016/j.jeurceramsoc.2021.11.064
22. J. L. Cardoso, A. L. S. N. Cavalcante, R. C. A. Vieira, P. de Lima-Neto, M. J. G. da Silva, Pitting corrosion resistance of austenitic and superaustenitic stainless steels in aqueous medium of NaCl and H_2SO_4, *Journal of Materials Research*, **31**, 1755 (2016). Doi: https://doi.org/10.1557/jmr.2016.198
23. M. Rahimian, N. Ehsani, N. Parvin, H. reza Baharvandi, The effect of particle size, sintering temperature and sintering time on the properties of Al–Al_2O_3 composites, made by powder metallurgy, *Journal of Materials Processing Technology*, **209**, 5387 (2009). Doi: https://doi.org/10.1016/j.jmatprotec.2009.04.007
24. E.-S.M. Sherif, Corrosion behavior of magnesium in naturally aerated stagnant seawater and 3.5% sodium chloride solutions, *International Journal of Electrochemical Science*, **7**, 4235 (2012). Doi: https://doi.org/10.1016/S1452-3981(23)19534-4
25. M. Knapek, M. Zemková, A. Greš, E. Jablonská, F. Lukáč, R. Král, J. Bohlen, P. Minárik, Corrosion and mechanical properties of a novel biomedical WN43 mag-

nesium alloy prepared by spark plasma sintering, *Journal of Magnesium and Alloys*, **9,** 853 (2021). Doi: https://doi.org/10.1016/j.jma.2020.12.017

26. J. Han, Y. Li, C Ma, Q. Zheng, X. Zhang, X. Wu, Study on the oxidation mechanism of Al-SiC composite at elevated temperature, *International Journal of Minerals, Metallurgy and Materials*, **31**, 2077 (2024). Doi: https://doi.org/10.1007/s12613-023-2778-3
27. J. Kim, and C. Jeong, Investigation of functional 6061 aluminum alloy oxide film with anodization voltage and its corrosion resistance, *Corrosion Science Technology*, **22**, 399 (2023). Doi: https://doi.org/10.14773/cst.2023.22.6.399
28. W. Kang, Corrosion Behavior of Silicon Carbide/7091 Aluminum Matrix Composites, *Corrosion Science and Technology*, **11**, 108 (2012). Doi: https://doi.org/10.14773/cst.2012.11.4.108